Single- and Multiple-RF Load Controlled Parasitic Antenna Arrays Operating at Cm-Wave Frequencies: Design and Applications for 5G Wireless Access / Backhaul

Konstantinos Ntougias, Dimitrios Ntaikos, Constantinos B. Papadias
Athens Information Technology (AIT), 44 Kifissias Avenue, 15125 Maroussi, Greece.
{kontou, dint, cpap}@ait.gr

***Abstract*—MIMO technology is expected to play a key role in the endeavour to reach the capacity target of 5G systems, in conjunction with the use of frequencies above 6 GHz. This communication paradigm is anticipated to be utilised also in the wireless backhaul domain, in order to meet the high capacity requirements of the future wireless transport networks. The performance of the considered MIMO transmission methods is determined by the number of antennas that can be deployed on the transmitting nodes, which in turn is limited by cost and energy consumption constraints. Load controlled parasitic antenna arrays represent a type of antenna systems which are able to boost the performance of these communication schemes, while employing a small number of antennas. In this paper, we present the design of single- and multiple-fed parasitic antenna arrays operating at the 19 GHz frequency band. Moreover, we describe a simple and robust technique that allows us to perform arbitrary channel-dependent precoding with such arrays. Furthermore, we study a low-complexity communication protocol that can be applied to setups that are equipped with such antenna systems and used in low-mobility scenarios, such as wireless backhaul applications. The numerical simulation results showcase the validity of these approaches for both wireless access and backhaul applications and demonstrate the superiority of the parasitic antenna arrays over equivalent, regarding the number of their antenna elements, antenna systems.**

***Index Terms*—Coordinated multiple-input multiple-output (Co-MIMO), channel state information (CSI), linear precoding, load-controlled parasitic antenna array (LC-PAA), wireless backhaul.**

I. Introduction

Fifth generation (5G) cellular mobile radio communications systems are expected to provide $1,000$ - $10,000$ greater capacity in the downlink (DL) than current fourth generation (4G) networks [1]. To this end, it is required the allocation of additional spectral resources to the envisioned bandwidth-demanding services. However, the segment of the radio spectrum below 6 GHz, which is traditionally used for the achievement of long-range wireless communications, is severely congested [2]. Therefore, the community has proposed a number of alternative radio access technologies (RAT), in order to address the spectrum crunch issue [3].

One trend is the use of centimetre-wave (cm-wave) and millimetre-wave (mm-wave) frequencies, since these spectral regions provide an abundance of unexploited bandwidth (BW) [4]. The use of such high frequencies, though, suits only short-range, low mobility, data-hungry applications [4].

Another direction is the densification of the radio access network (RAN), i.e. the deployment of a large number of small cells across the service area, so that the system capacity is increased through aggressive frequency re-use [5]. Nevertheless, this approach leads to severe inter-cell interference (ICI) which has the potential to degrade the quality-of-service (QoS) of the cell-edge users and limit the overall capacity [5]. Therefore, the use of sophisticated ICI management techniques is required [5].

Multiple-input multiple-output (MIMO) technology constitutes another example. MIMO communication schemes leverage the spatial dimension provided by the utilisation of multiple antennas at the transmitting nodes and possibly at the receiving ones, i.e. at the base stations (BS) and the user terminals (UT) respectively, in order to increase the spectral efficiency (SE) of the system without any extra cost in terms of transmission power or BW [6]. More specifically, these transmission methods enable the spatial multiplexing (SM) of a number of radio signals (i.e. the concurrent transmission of multiple data signals on the same frequency) destined either to a single user or to a group of individual users [6]. The former paradigm is known as single-user MIMO (SU-MIMO), while the latter one is referred to as multi-user MIMO (MU-MIMO).

MU-MIMO has gained popularity over SU-MIMO lately, since, in contrast to the latter paradigm, (a) it enables the spatial sharing of the spectral resources among a set of active users; and (b) it does not require the installation of multiple antennas at the UTs, which is problematic due to size, cost, and energy consumption constraints [7]. In order to reduce or even eliminate the corresponding intra-cell co-channel interference (CCI), which is also known as multi-user interference (MUI), MU-MIMO relies on the application of appropriate precoding schemes [6]. Precoding, in turn, requires the availability of channel state information (CSI) at the transmitting node (i.e. the BS) [6].

Coordinated MIMO (Co-MIMO) is an extension of MU-MIMO that emerged recently. This technology facilitates uni-

versal frequency re-use by mitigating the resulting ICI [8]. Co-MIMO is based to this end on the cooperation between neighbouring BSs, which is expressed via the exchange of their beamforming (BF) vectors / precoding matrices, possibly along with control information such as their power allocation vectors and user scheduling sets, CSI, the user data, or combinations thereof [8]. The most common "flavours" of Co-MIMO are coordinated scheduling / coordinated BF (CS/CBF), where there is no data sharing and the cooperating nodes coordinate their transmissions in order to reduce the ICI; and joint transmission (JT), where the cooperating BSs share the user data and jointly serve the scheduled cell-edge users, thus turning the interfering signals into data signals and, therefore, eliminating the ICI and further enhancing the system performance [8]. The various "flavours" of Co-MIMO differ on their performance gain over non-coordinated MIMO variants as well as on the burden that they place on the transport network [8].

Given the high capacity requirements of the transport network, which are attributed to the use of multiple antenna communications techniques and the utilisation of cm-wave / mm-wave RATs, it is considered lately the adoption of the MU-MIMO and Co-MIMO paradigms, wherever possible, by the wireless backhaul [9].

The performance of the aforementioned MIMO transmission schemes depends on the degrees-of-freedom (DoF) provided by the antenna systems that are installed on the transmitting nodes [6][7]. Typically, digital antenna arrays (DAA) are utilised. These antenna systems make use of active (i.e. voltage-driven) elements. Thus, the array DoF equal the number of deployed antennas [6][7]. However, since each antenna should be connected to a radio frequency (RF) chain, the cost, complexity, and energy consumption grow with the number of antenna elements [7]. Moreover, if the antennas are closely spaced, the resulting electromagnetic coupling among them reduces the radiation efficiency of the antenna system [7]. These limitations prohibit the use of a high number of antennas in practice and, therefore, do not allow us to fully exploit the potential of the MIMO communication methods described above [7].

As a consequence, there is a growing interest lately on hybrid analogue-digital arrays that address these issues. Load-controlled parasitic antenna arrays (LC-PAA) represent a characteristic example. These compact antenna systems employ a limited number of active antenna elements. These antennas are surrounded by passive antenna elements that are terminated to tunable loads. Due to the strong mutual coupling, which is caused by the deliberately chosen small antenna spacing, the feeding voltages induce currents on the ports of the so-called parasitic antennas. By adjusting the loading values, we can control accordingly the currents that run on the parasitic antennas [7]. Thus, we can perform adaptive BF [10]. This is possible even when the LC-PAA has a single RF, since the exploitation of the mutual coupling allows a LC-PAA to provide more DoF than a corresponding DAA with the same number of RF modules. Alternatively, a LC-PAA may provide the same DoF as a DAA with more RF units. Hence, LC-PAAs lead to cost, complexity, and energy consumption savings or to performance improvement, respectively [7].

It was shown recently that LC-PAAs can perform also channel-dependent precoding [11], thus paving the way for using this technology in MU-MIMO / Co-MIMO setups. The technique described in [11] refers to the mapping of the precoded signals on the antenna currents and the calculation of the corresponding loading values that will generate these currents.

In dense urban environments where the backhaul nodes (BN) are often compact, low-cost, low-power small-cell base stations (SBS) or remote radio heads (RRH), the use of such simple, low-cost antenna arrays that generate relatively wide beams in conjunction with the utilization of MU-MIMO / Co-MIMO to enhance the SE and and mitigate the CCI is a promising alternative against the standard wireless backhauling practice of using complex, high-cost, highly directive antennas.

In addition, the use of wider beams may provide flexibility to the backhaul system, since in this case the effect of scattering is not negligible and may assist in link establishment, which is important in dense small-cell networks (SCN) where often there is no line-of-sight (LoS) path available or when an alternative route should be established "on-the-fly" due to some link / BN failure.

Also, the use of a limited number of RF chains reduces the CSI feedback overhead. (Recall that channel-dependent precoding requires CSI at the TX (CSIT)).

However, the method presented in [11] does not support any arbitrary precoding scheme or input signal constellation, since the required loading values may result in system instability [11]. A workaround is proposed in [12]. This method relies on the use of the optimum approximation of the input signal, in terms of the mean square error (MSE), instead of the original data signal, in order to generate the required antenna currents with a feasible loading set that will not lead to system instability. Nevertheless, this approach is not robust [12]. In addition, it presents high computational complexity, which discourages its application in practice [12].

In this work, we present the design of LC-PAAs operating at the 19 GHz as well as their use in cellular wireless access and backhaul applications. More specifically, we present a simple, robust, arbitrary channel-dependent precoding method and a low-complexity communication protocol that can be applied in low-mobility scenarios such as wireless backhauling. We complement our analysis with numerical simulations in order to obtain useful insights.

The structure of the remainder of the paper is as follows: Sec. II provides a short introduction to MU-MIMO and Co-MIMO. Sec. III presents the channel-dependent framework for LC-PAAs. Sec. IV describes the low-complexity communication protocol. Sec. V deals with the design of LC-PAAs at cm-wave frequencies. Both single-fed and multiple-active multiple-passive (MAMP) arrays are considered. Sec. VI

presents the results of the numerical simulations. Finally, Sec. VII provides the conclusions of our study.

II. Multi-User and Coordinated MIMO

A. MU-MIMO: System Model

In MU-MIMO, the BS serves a set of users over a resulting point-to-multipoint (PTMP) channel which is referred to as the MIMO broadcast channel (MIMO-BC) [6]. A suitable performance measure for MU-MIMO systems is the sum-rate (SR) capacity, which is the maximum of the sum of all possible user rate combinations [6]. The average SR capacity of the MIMO-BC scales linearly with the minimum of the number of antennas installed at the BS and the total number of antennas at the UTs [6][7]. Hence, when there are at least as many users as transmit antennas, the average SR capacity grows with the number of service antennas, irrespective of the number of antennas installed at each UT [6][7]. These statements hold also in the high signal-to-noise-ratio (SNR) regime. In the low-SNR regime, on the other hand, the optimal strategy is to schedule a single user (the one with the best channel) and apply transmit BF, since then the BF gain is translated into a linear capacity gain [6][7].

The capacity-achieving transmission strategy is dirty paper coding (DPC), a multi-user encoding scheme that takes advantage of the non-causal knowledge of the MUI to subtract it prior to transmission [6]. However, its high computational complexity attributed to the use of successive encodings and decodings turn this non-linear pre-processing method practically infeasible, especially when the user population is large [6].

Linear precoding constitutes a suboptimal alternative that offers a good compromise between performance and complexity. This technique leverages the physical separation of the users to enable the spatial sharing of the channel through the application of multi-stream transmit BF [6].

The input-output relationship of a $(M,(K,1))$ Multiple-Input Single-Output Broadcast Channel (MISO-BC) formed between a BS with M transmit antennas and K single-antenna UTs, assuming that linear precoding is utilized and that the channel is modeled as a quasi-static flat-fading channel, is given by [6]

$$y = \mathbf{h}^{\dagger}\left(\sum_{m=1}^{K}\mathbf{w}_m\sqrt{p_m}s_m\right)+n, \quad k=1,2,\ldots,K \tag{1a}$$

$$\mathbf{y} = \mathbf{H}\mathbf{W}\mathbf{P}^{1/2}\mathbf{s}+\mathbf{n}, \tag{1b}$$

where $\mathbf{y}$ is a $(K\times 1)$ vector whose element y_k is the received signal at the kth user; $\mathbf{H}$ denotes the $(K\times M)$ channel matrix, whose rows $\mathbf{h}_k$ are $(1\times M)$ vectors that hold the channels h_{km} between the kth user and each one of the M transmit antennas; $\mathbf{W}$ represents the $(M\times K)$ precoding matrix, whose column $\mathbf{w}_k$ is the $(M\times 1)$ BF vector for the kth user; $\mathbf{P}$ is the $(K\times K)$ power allocation matrix, whose element p_k is the power allocated to the kth user; $\mathbf{s}$ refers to the $(K\times 1)$ symbol vector, with s_k being the data symbol intended for the kth user; and $\mathbf{n}$ is the $(K\times 1)$ additive noise vector, whose elements n_k represent the noise at the kth receiver.

The signal-to-interference-plus-noise-ratio (SINR) at the kth user is expressed as [6]

$$\text{SINR}_k = \frac{\left|\mathbf{h}_k^{\dagger}\mathbf{w}_k\right|^2 p_k}{\sum_{m\neq k}\left|\mathbf{h}_k^{\dagger}\mathbf{w}_m\right|^2 p_m+\sigma_n^2}, \quad k=1,2,\ldots,K, \tag{2}$$

where σ_n^2 is the noise variance. The data rate of that user is [6]

$$R_k = \log_2\left(1+\text{SINR}_k\right), \tag{3}$$

and the sum-rate (SR) throughput is given by [6]

$$R = \sum_{i=1}^{K}R_k = \sum_{i=1}^{K}\log_2\left(1+\text{SINR}_k\right). \tag{4}$$

B. MU-MIMO: Linear Precoding Schemes

Several variants of linear precoding exist. Zero Forcing BF (ZFBF) makes use of BF vectors that are orthogonal to the subspace of other users' channel vectors in order to eliminate the MUI. That is, the inner product of a user's BF vector with other users' channel vectors is zero [13]:

$$\left\|\mathbf{h}_k^{\dagger}\mathbf{w}_m^{(\text{ZF})}\right\|^2 = 0, \quad k,m=1,2,\ldots,K,\ m\neq k. \tag{5}$$

The ZF condition is translated into the use of the Moore-Penrose pseudo-inverse of the composite channel matrix as the precoding matrix [13]:

$$\mathbf{F}^{(\text{ZF})} = \mathbf{H}^{+} = \mathbf{H}^{\dagger}\left(\mathbf{H}\mathbf{H}^{\dagger}\right)^{-1}. \tag{6a}$$

$$\mathbf{W}^{(\text{ZF})} = \frac{\mathbf{F}^{(\text{ZF})}(:,k)}{\|\mathbf{F}^{(\text{ZF})}(:,k)\|}, \quad k=1,2,\ldots,K. \tag{6b}$$

This precoding scheme attains a significant portion of the DPC capacity in the high SNR regime, especially when single-antenna terminals are utilized [6]. Also, it approaches the capacity as the number of users grows towards infinity, since in this case user scheduling benefits from the abundance of spatial directions and the multi-user diversity effect [6]. On the other hand, though, ZFBF is power-inefficient, since the BF vectors do not match to the users' channels. Thus, ZFBF performs poorly at low SNR values [6].

Regularised ZFBF (RZFBF) is an extension of ZFBF that introduces a controllable amount of MUI at the cell. The value of the coefficient that controls the level of the residual MUI is typically set such that the SINR at the users is maximized. More specifically, in RZFBF we have [13]

$$\mathbf{v}_k^{(\text{RZF})} = \mathbf{H}^{\dagger}\left(\frac{1}{p_k}\mathbf{I}_K+\mathbf{H}\mathbf{H}^{\dagger}\right)^{-1}, \quad k=1,2,\ldots,K. \tag{7a}$$

$$\mathbf{w}_k^{(\text{RZF})} = \frac{\mathbf{v}_k^{(\text{RZF})}}{\|\mathbf{v}_k^{(\text{RZF})}\|}, \quad k=1,2,\ldots,K. \tag{7b}$$

RZFBF is asymptotically optimal at both low and high SNR and outperforms ZFBF at intermediate SNR values [15]. However, the power allocation process is more complex due to the residual MUI.

Once a linear precoding scheme has been chosen, the optimization of the system's performance, in terms of the achieved average SR throughput, depends on the employed user selection and power allocation schemes.

C. Power Allocation Scheme

Our goal is to maximize the SR throughput under per-antenna transmission power constraints. This optimization problem is expressed mathematically as follows:

$$\begin{aligned} \underset{p_k>0}{\text{maximize}} \quad & R = \sum_{k=1}^{K} \log_2\left(1+\text{SINR}_k\right) \\ \text{subject to} \quad & p_k \leq P. \end{aligned} \tag{8}$$

After fixing the precoder, we obtain the following water-filling power allocation (WF-PA) solution to the aforementioned problem [14]:

$$p_k = \left[\upsilon_k - \frac{\sigma_n^2}{\overline{h}_k}\right]^+, \tag{9}$$

where υ_k is the water level, $\overline{h}_k$ is the effective channel after precoding, and $[x]^+ = \max(x, 0)$.

D. Coordinated MIMO

In Co-MIMO, extensions / generalizations of the linear precoding schemes described in Sec. II-B are utilised [8]. Moreover, in JT, the channel is modeled as a "super MISO-BC", since the cooperating BSs form effectively a composite node serving all the scheduled users [8].

III. Simple Robust Arbitrary Channel-Dependent Precoding with Single-Fed LC-PAAs

Fig. 1 shows the equivalent circuit diagram of a M-element single-fed LC-PAA whose $(M-1)$ parasitic elements are connected to tunable loads with purely imaginary impedance (e.g. varactor diodes). The relation between the currents and voltages associated with the antenna elements is given by the generalized Ohm's law as [11]

$$\mathbf{i} = \left(\mathbf{Z} + \mathbf{Z}_L\right)^{-1} \mathbf{v}, \tag{10}$$

where $\mathbf{i}$ is the $(M \times 1)$ vector of the currents that run on the antenna elements; $\mathbf{Z}$ is the $(M \times M)$ mutual coupling matrix whose diagonal entry Z_{mm} represents the self-impedance of the mth antenna element while the off-diagonal entry Z_{mk} denotes the mutual impedance between the mth and the kth antenna element; $\mathbf{Z}_L$ is the $(M \times M)$ diagonal load matrix whose diagonal elements are the source resistance R_s and the impedances of the parasitic loads jX_m $(m = 2, 3, \ldots, M)$, with $j = \sqrt{-1}$ denoting the imaginary unit; and $\mathbf{v}$ is the $(M \times 1)$ voltage vector that holds the sole feeding voltage v_s. Note that $\mathbf{Z}$ depends on the geometry of the array and it is typically measured or it is calculated with the help of appropriate computer software.

The system model of a (M, N) MIMO link established between a TX and a RX having M and N antennas, respectively, is given from an antenna perspective by [11]

$$\mathbf{y} = \mathbf{H}\mathbf{i} + \mathbf{n}, \tag{11}$$

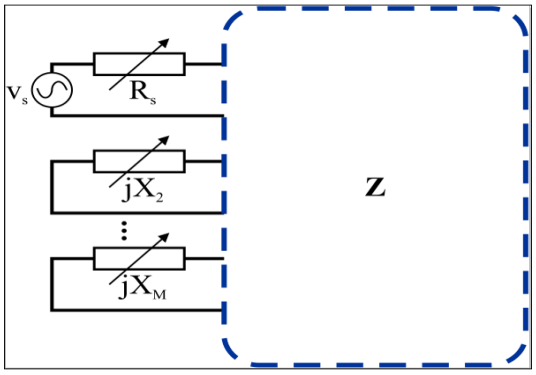

Fig. 1. Equivalent circuit diagram of a single-fed load-controlled parasitic antenna array.

where $\mathbf{y}$ is the $(N \times 1)$ vector of open-circuit voltages at the receive antennas, $\mathbf{i}$ represents the $(M \times 1)$ vector of currents that run on the transmit antennas, $\mathbf{H}$ denotes the $(N \times M)$ channel matrix whose entry h_{nm} relates the mth input current with the nth open-circuit output voltage, and $\mathbf{n}$ constitutes a $(N \times 1)$ AWGN vector with covariance matrix $\mathbf{R}_n = \mathbb{E}\left(\mathbf{n}\mathbf{n}^\dagger\right) = \sigma_n^2 \mathbf{I}_N$. Note that the same relation holds also for the case of MU-MIMO, where the N receive antennas are shared by K users.

Assuming the application of linear precoding, the input-output signal relationship in Eq. (11) becomes

$$\mathbf{y} = \mathbf{H}\mathbf{W}\mathbf{s} + \mathbf{n}, \tag{12}$$

where $\mathbf{W}$ is the $(M \times M)$ precoding matrix and $\mathbf{s}$ is the $(M \times 1)$ input signal vector. (We have omitted the power allocation matrix for convenience.) Hence, in order to apply channel-dependent precoding to a single-fed LC-PAA, we have to map the precoded symbols to the antenna currents as follows [15]:

$$\mathbf{i} = \mathbf{W}\mathbf{s}. \tag{13}$$

Then, we have to compute the loading values that will give rise to the required currents according to Eq. (10) under the constraint of a positive input resistance, in order to ensure that the antenna system will not reflect power back, thus leading to system instability [16]. However, this design condition cannot be met for any given input signal constellation or precoding scheme.

On the other hand, single-fed LC-PAAs can admit any input signal in transmit BF applications, since the array manifold required to shape the radiation pattern as desired does not depend on the format of the input signal. The role of the parasitic loads in this case is to generate currents with appropriate magnitude and phase shift, so that the desired beam is produced. This is similar with the functionality of BF weights in conventional antenna arrays. The only precondition that has to be met is that the impedances of the loads should take values within a reasonable range.

Based on this remark, we suggest a simple alternative approach for performing robust, arbitrary channel-dependent precoding with single-fed LC-PAAs [13]:

1) First, we apply transmit BF using any valid method.
2) Then, we perform channel-dependent precoding over the employed beam.

By taking advantage of the radiation pattern's reconfiguration capabilities of single-fed LC-PAAs through the decoupling of the problem to a BF and a precoding part, we overcome the aforementioned circuit stability and implementation complexity issues. The extension of this approach for MAMP arrays is trivial.

IV. A Low-Complexity Communication Protocol for Low-Mobility Scenarios

The computational complexity related with the dynamic calculation of the parasitic loads' impedances discourages the application of the LC-PAA technology in real systems. Moreover, the beam tracking procedure required in practice to ensure mobility support is fairly complex, especially as we move to higher frequencies where typically the beams are narrower, regardless of the type of antenna system employed.

In this Section, we describe a low-complexity communication protocol for MU-MIMO / Co-MIMO systems equipped with LC-PAAs, which can be utilized in low-mobility or static scenarios and addresses the aforementioned issues. More specifically, we assume that instead of tunable loads, the LC-PAAs make use of a number of fixed loading sets. Each one of them corresponds to a predetermined radiation pattern (i.e. a beam). A simple RF switch allows us to connect the passive antenna elements to the desired loading set. Thus, we utilise beam switching through loading set switching.

The system operation is divided in three phases [13]:

1) **Learning phase:** For each beam combination, the BS(s) sends a pilot signal. Then, the UTs measure their SINR or estimate the gain of the direct and cross channels and report back this channel quality metric.
2) **Beam-selection phase:** After switching through all possible beam combinations, the BS(s) selects the optimum one, in terms of the achieved SR throughput, based on the information reported by the UT.
3) **Transmission phase:** The BS(s) transmits over the selected beams.

The use of fixed beams reduces the complexity of load calculation and beam tracking. Moreover, the use of SINR feedback further reduces complexity, since it is commonly much easier to measure the SINR than to estimate the gain of a number of channels. After SINR-feedback-based beam selection, a CSI-feedback procedure for the composite channel formed by the selected beam combination takes place, in order to enable the use of precoding.

V. Design of LC-PAAs

A. 19.25GHz bowtie parasitic antenna array

Migrating to frequencies in the K-band with the use of parasitic antennas is a fairly difficult task. Even a slight change in the dimensions of the elements (both active and parasitic) has a large impact in the resonant frequency and / or the radiation pattern shape. This section presents our initial simulated results of a K-band (19.25GHz) parasitic antenna. In Figure 3 we present the initial design of the bowtie parasitic antenna array, resonating at 19.25GHz. It consists of one active and ten parasitic elements, that have a bowtie-like shape. The active element is located at the center of the dielectric board (indicated as RF) and it is surrounded by the parasitic elements (indicated with a sequential number). Note that in the middle of each printed parasitic element (printed bowtie) there is a small gap, where the loads (capacitors or inductors) are placed.

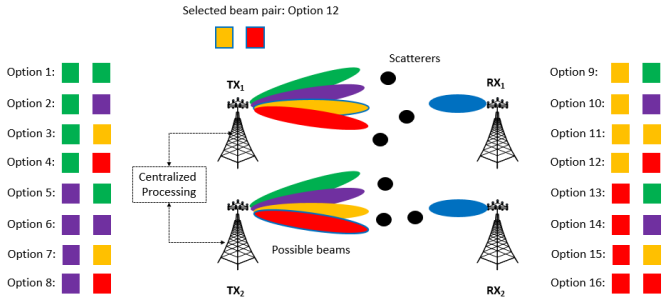

Fig. 2. A Co-MIMO system comprised by 2 transmit and 2 receive nodes equipped with single-fed LC-PAAs. Each transmit LC-PAA can generate at each time one out of four different beams. The best beam combination is selected jointly by the transmitters, based on SINR or CSI feedback from the receivers. Then, precoded transmission takes place over these beams.

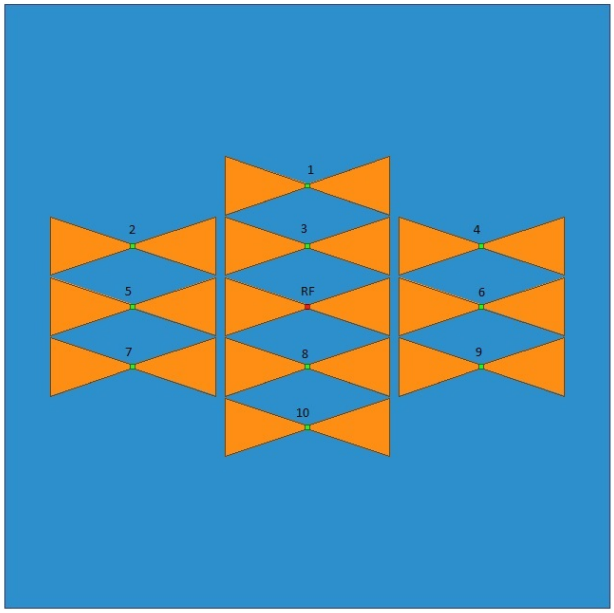

Fig. 3. Initial prototype design of the bowtie planar antenna at 19.25GHz.

The actual values of the loads that were used for the simulation, along with their equivalent Ohmic resistance at 19.25GHz are presented in Table I.

In Figure 4 we present the scattering parameters versus frequency (4a) and the three main planes of the far field radiation pattern (Figures 4b, 4c and 4d). It should be noted

TABLE I
Calculated load values for the 19.25GHz bowtie parasitic antenna.

Element number	Capacitor or Inductor value	Impedance at 19.25GHz
1	41.34pH	X_L = 5.0 Ohms
2	41.34pH	X_L = 5.0 Ohms
3	45.47pH	X_L = 5.5 Ohms
4	41.34pH	X_L = 5.0 Ohms
5	0.275pF	X_C = 30 Ohms
6	0.275pF	X_C = 30 Ohms
7	0.275pF	X_C = 30 Ohms
8	0.275pF	X_C = 30 Ohms
9	0.275pF	X_C = 30 Ohms
10	0.275pF	X_C = 30 Ohms

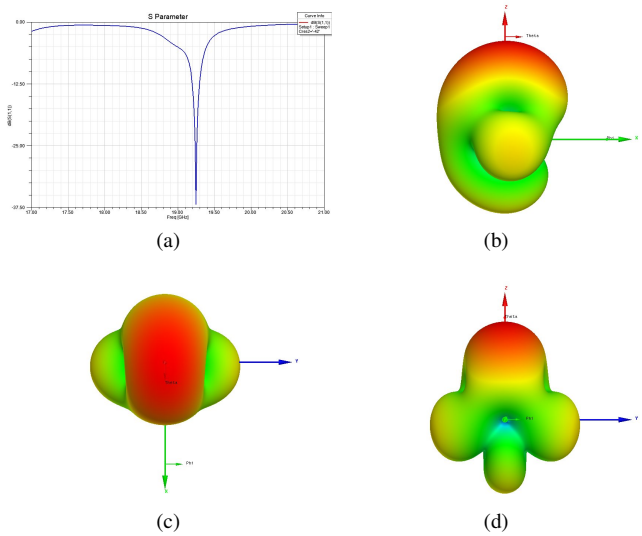

Fig. 4. (a) S-parameters vs frequency. The three main plains of the far field radiation pattern. (b) x-z, (c) x-y, (d) y-z.

that the main lobe has a half power beam width (HPBW) of around 38° and a gain of 9dBi. Considering that the active element is similar to a dipole, thus having a donut-like far-field radiation pattern with a gain of 0dBi, it is quite impressive that by carefully placing the loaded parasitic elements, we confined the far-field radiation pattern to less than 40°, while at the same time boosting its gain to 9dBi.

B. 19.37GHz MAMP parasitic antenna

In order to create a MAMP (multiple - active multiple - passive) parasitic antenna, in this section we combine four of the parasitic bowtie antennas (groups) presented in V-A. Small changes to inter-element distances had to be made in order to preserve the operational frequency at about the same resonant frequency as before (in this case there is a small increase in the resonant frequency, which will be alleviated through more accurate simulations). Note that all the relevant load values are the same (per group) as the ones described in Table I. In Figure 5 we present the initial design of the MAMP parasitic antenna array, resonating at 19.37GHz. It consists of

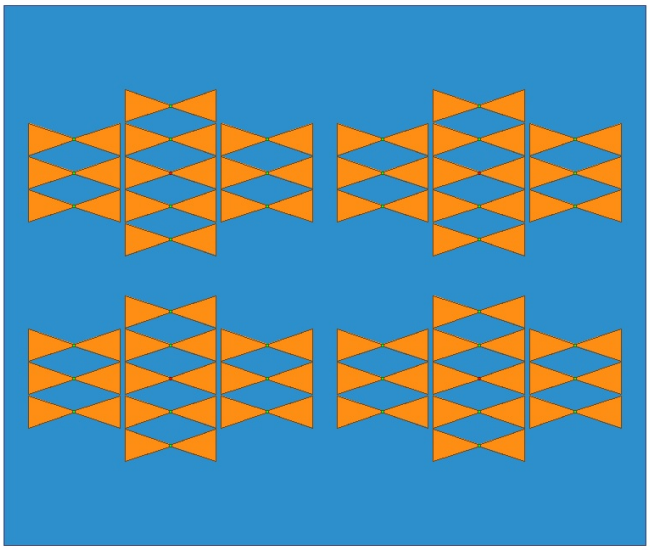

Fig. 5. Initial prototype design of the MAMP planar antenna.

four groups of one active and ten parasitic elements, leading to a design with four active and fourty parasitic elements.

In Figure 6 we present the scattering parameters versus frequency (Figure 6a), and the 3D far field radiation pattern (Figure 6b). It should be noted that the main lobe has a half power beam width (HPBW) of around 35° and a gain of 6dBi.

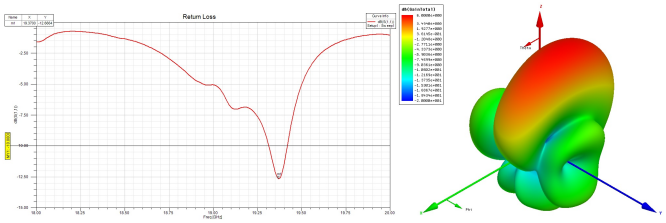

Fig. 6. (a) S-parameters vs frequency and (b) the 3D far field radiation pattern.

VI. Numerical Simulations and Performance Evaluation

In this Section, we evaluate the performance of the proposed arbitrary precoding framework and low-overhead communication protocol for various MIMO setups through a number of numerical simulations. We compare the case where the nodes are equipped with LC-PAAs against the scenario where equivalent DAAs are installed on them. The target SNR range is [0 dB, 30 dB]. The results refer to the average SR throughput obtained after 100 simulation runs. The simulation is based on a realistic scattering environment. The radiation patterns have been generated from appropriate antenna design software.

In Fig. (7) the performance of a $(4,(4,1))$ MU-MIMO wireless access system equipped with a LC-PAA vs. the one of a corresponding system equipped with an equivalent DAA

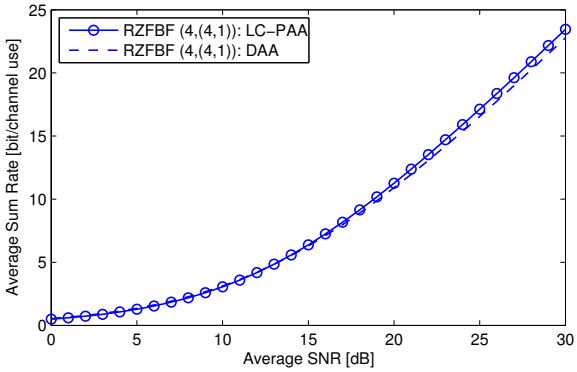

Fig. 7. SR throughput of $(4,(4,1))$ systems utilizing RZFBF. Each system is equipped with either a LC-PAA or a DAA and operates at the 19 GHz band.

is illustrated. The RZFBF scheme is utilised. We note that the LC-PAA-equipped system outperforms slightly its DAA counterpart at high SNR.

In Fig. 8 the performance of the wireless backhaul system setup shown in Fig. 2 is depicted. The considered scenarios include beam pair selection based on SINR feedback and on CSI feedback. In the former case, the use of ZFBF is assumed, while in the latter one both ZFBF and RZFBF techniques are considered. The employed Co-MIMO variant is JT. We note that beam pair selection based on CSI feedback improves significantly the performance of ZFBF. Also, RZF outperforms ZFBF in low SNR values, as expected.

VII. Conclusion

In this paper, we described the design of single- and multi-RF LC-PAAs that operate at the 19 GHz frequency band. We presented also an approach that enables us to perform simple, robust, arbitrary channel-dependent linear precoding with such arrays as well as a low-complexity communication protocol that can be applied in low-mobility scenarios. Finally, we evaluated various precoding methods applied in both MU-MIMO and Co-MIMO setups equipped with LC-PAAs via numerical simulations. The simulation results not only showcase the validity of the proposed techniques and their potential to be used in wireless access and backhaul applications but they also demonstrate that the LC-PAAs outperform equivalent (regarding the number of their RF chains) DAAs.

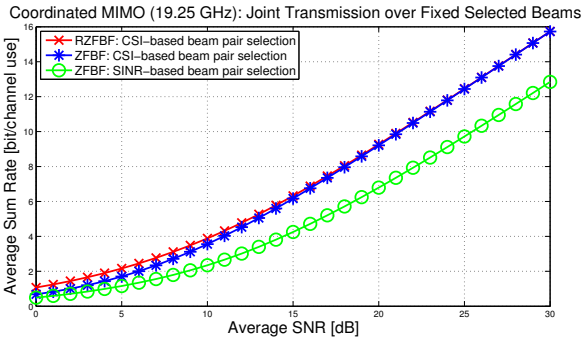

Fig. 8. Performance of the communication protocol described in Sec. IV.

References

[1] "Assessment of the Global Mobile Deployments and Forecasts for International Mobile Telecommunications," ITU-R, Report M.2243, November 2011.

[2] M. Mueck *et al.*, "Novel Spectrum Usage Paradigms for 5G," IEEE SIG CR in 5G, White Paper, November 2014.

[3] "5G Vision," 5G-PPP, Tech. Rep., February 2015.

[4] T. Rappaport *et al.*, *Millimeter Wave Wireless Communications*. Prentice Hall, 2015.

[5] A. Osseiran *et al.*, Eds., *5G Mobile and Wireless Communications Technology*. Cambridge University Press, 2016.

[6] H. Huang *et al.*, Eds., *MIMO Communication for Cellular Networks*. Springer-Verlag New York, 2001.

[7] A. Kalis *et al.*, Eds., *Parasitic Antenna Arrays for Wireless MIMO Systems*. Springer-Verlag New York, 2014.

[8] D. Lee *et al.*, "Coordinated Multipoint Transmission and Reception in LTE-Advanced: Deployment Scenarios and Operational Challenges," *IEEE Communications Magazine*, vol. 50, no. 2, pp. 148–155, February 2012.

[9] Shared Access Terrestrial-Satellite Backhaul Network enabled by Smart Antennas (SANSA H2020). [Online]. Available: http://www.sansa-h2020.eu/

[10] T. Ohira and K. Gyoda, "Electronically Steerable Passive Array Radiator Antennas for Low-Cost Analog Adaptive Beamforming," in *IEEE International Conference on Phased Array Systems and Technology*, 2000, pp. 101–104.

[11] V. Barousis *et al.*, "A New Signal Model for MIMO Communications with Compact Parasitic Arrays," in *IEEE International Symposium on Communications, Control and Signal Processing*, Athens, Greece, May 21-23 2014, pp. 109–113.

[12] L. Zhou *et al.*, "Achieving arbitrary signals transmission using a single radio frequency chain," *IEEE Transactions on Communications*, vol. 63, no. 12, pp. 4865–4878, October 2015.

[13] K. Ntougias *et al.*, "Coordinated MIMO with Single-fed Load-Controlled Parasitic Antenna Arrays," in *17th IEEE International Workshop on Signal Processing advances in Wireless Communications (SPAWC 2016)*, Edinburgh, UK, July 3-6 2016, pp. 1–5.

[14] E. Bjornson and E. Jorswieck, "Optimal Resource Allocation in Coordinated Multi-Cell Systems," *Foundations and Trends in Communications and Information Theory*, vol. 9, no. 2-3, pp. 113–381, January 2013.

[15] G. Alexandropoulos *et al.*, "Precoding for multiuser mimo systems with single-fed parasitic antenna arrays," in *IEEE Global Communications Conference (GLOBECOM)*, Austin, TX, USA, December 8-12 2014, pp. 3897–3902.

[16] V. Barousis and C. B. Papadias, "Arbitrary precoding with single-fed parasitic arrays: Closed-form expressions and design guidelines," *IEEE Wireless Communications Letters*, vol. 3, no. 2, pp. 229–232, February 2014.